

Heat transfer analysis of pile geothermal heat exchangers with spiral coils

Ping Cui^{a,b,c,*}, Xin Li^c, Yi Man^c, Zhaohong Fang^b

^aKey Laboratory of Renewable Energy Utilization Technologies in Buildings, Ministry of Education, Jinan, China

^bSchool of Thermal Energy Engineering, Shandong Jianzhu University, Jinan, China

^cShandong Key Laboratory of Building Energy-saving Technique, Jinan, China

ARTICLE INFO

Article history:

Received 26 September 2010

Received in revised form 22 February 2011

Accepted 29 March 2011

Available online 20 April 2011

Keywords:

Ground-coupled heat pump

Pile geothermal heat exchanger

Heat transfer

Spiral coil

Ring-coil source

ABSTRACT

This paper investigates the transient heat conduction around the buried spiral coils which could be applied in the ground-coupled heat pump systems with the pile foundation as a geothermal heat exchanger. A transient ring-coil heat source model is developed, and the explicit analytical solutions for the temperature response are derived by means of the Green's function theory and the image method. The influences of the coil pitch and locations are evaluated and discussed according to the solutions. In addition, comparisons between the ring-coil and cylindrical source models give that the improved finite ring-coil source model can accurately describe the heat transfer process of the pile geothermal heat exchanger (PGHE). The analytical solutions may provide a desirable and better tool for the PGHE simulation/design.

© 2011 Elsevier Ltd. All rights reserved.

1. Introduction

The ground-coupled heat pump (GCHP) technology is one of the most energy efficient ways to provide both space heating and cooling for buildings because the underground environment experiences less temperature fluctuation than the ambient air temperature. In a GCHP system, heat is extracted from or rejected to the ground via a geothermal heat exchanger (GHE) through which pure water or anti-freezing solution circulates. The commonly used GHE in closed loop systems typically consists of high-density polyethylene (HDPE) U-tubes installed in vertical boreholes which are called vertical GCHP systems. A number of vertical GCHP systems have been installed around the world including in China due to the increasing awareness of environmental issues and growing energy crisis [1,2]. However, the main restriction against the GCHP application in urban areas is that the system requires a large plot of land for installation of GHEs, and this is usually difficult in cities. Besides, larger GHEs significantly increase the initial cost of the GHE installation. Therefore, the high installation cost of excessively large GHEs and the limited urban land area have restricted to a large extent the wide applications of this technology in densely-populated areas.

Recently, a novel GHE system which utilizes the foundation piles of a building as the means of transferring heat to and from the ground has attracted great interest among researchers and

engineers in the GCHP industry. This new system is known as the "Pile Geothermal Heat Exchanger (PGHE) system". The piles can not only support the building structure but also act as heat exchangers. Each pile can carry a closed-loop pipe connected to a heat pump on the ground for heating, cooling and hot water supply. Pipes may be buried in concrete piles in configurations of U-tubes or spiral coils. The pile grout material, mainly concrete, provides good tight contact between the buried pipes and the piles and between the piles and the surrounding soil as well. Therefore it can significantly reduce the thermal contact resistance, and improve the heat transfer efficiency of the PGHE. The most competitive advantage of this system is the considerable reduction of the initial cost and the plot of land for the borehole field.

A few studies on PGHE systems have been recently reported in literature, mostly by either experiments or numerical simulations. Morino and Oka (1994) first employed steel piles, which were used for building foundations, as heat exchangers [3]. In their study, the heat transfer characteristics of the steel pile equipped with two vertical tubes were evaluated by means of experiments and a three-dimensional finite difference method. Pahud (1996) developed a simulation tool (called PileSIM) based on a TRNSYS environment for heating and cooling, which used heat exchanger piles with vertical U-tube pipes [4]. The simulation tool employed the Duct Ground Heat Storage Model (DST) which was solved by means of numerical methods. Later, a heat exchanger pile system was designed by using the simulation tool for heating and cooling a terminal building at Zurich Airport [5]. Laloui et al. (2006) studied the behaviors of a heat exchanger pile for thermo-mechanical loads, especially increased loads on the pile caused by thermal ef-

* Corresponding author at: Key Laboratory of Renewable Energy Utilization Technologies in Buildings, Ministry of Education, Jinan, China.

E-mail address: sdcuiping@gmail.com (P. Cui).

Nomenclature

a	thermal diffusivity ($\text{m}^2 \text{s}^{-1}$)
b	coil or spiral pitch (m)
B	dimensionless coil pitch
c	specific heat ($\text{J kg}^{-1} \text{K}^{-1}$)
$ Fo$	Fourier number
$h1, h2$	pile depth (m)
H	dimensionless depth
k	thermal conductivity ($\text{W m}^{-1} \text{K}^{-1}$)
q	heating rate (W)
q_l	heating rate per length (W m^{-1})
R	dimensionless radius
r	radial coordinate (m)
r_0	pile radius (m)
t	temperature ($^{\circ}\text{C}$)
t_0	initial temperature ($^{\circ}\text{C}$)
z	axial coordinate (m)

Z dimensionless coordinate

Greek symbols

θ	temperature excess ($^{\circ}\text{C}$)
Θ	dimensionless temperature excess
ρ	density (kg m^{-3})
τ	time (s)
φ	angular coordinate (rad)

Subscripts

c	cylindrical source
f	finite length
i	infinite length
r	ring-coil source
s	single ring-coil source

fects, using a coupled multi-physical finite element model [6]. Yasuhiro et al. (2007) investigated the field performance of a PGHE system using friction piles as heat exchangers for space heating which was built in Japan in 2000 [7]. Sekine et al. (2007) developed a GCHP system that utilized the cast-in-situ concrete pile foundation embedded in U-tubes as heat exchangers [8].

In the previous studies, the heat exchanger pipes in practice in the PGHE systems are U-tube pipes, including single, double, triple or even quadruple U-tubes. Few studies on the PGHE with spiral coils have been carried out due to the complexity of its heat transfer process. However, the spiral coil configuration has the advantages of more heat transfer area in a certain pile and better flow pattern without air chocking in the pipes compared with the serial or parallel U-tubes in the pile. In addition, the spiral coil system can reduce the complexity of the pipe connections and decrease to a certain extent the thermal “short-circuit” between supply and return pipes. The schematic diagram of a GCHP system with spiral coils buried in a pile foundation is illustrated in Fig. 1.

Due to its short application history and geometrical characteristics, few analytical models for the PGHE have been developed and

the models for the conventional boreholes are commonly used to give a rough estimation in the PGHE applications. However, the heat transfer characteristics of the PGHE system are quite different from those of conventional vertical boreholes. Piles are much thicker in diameter but shorter in depth than boreholes. The heat transfer coils are inside the pile concrete but disposed within about 10 cm of the pile's outer surface. Obviously, either the line source models [9–12] or the “hollow” cylindrical model [13] is no longer valid in this case due to their respective simplifying assumptions. Based on the classical models, our research group has recently proposed a new model, i.e. the “solid” cylindrical source model [14], and takes the PGHE characteristics into proper consideration, as shown in Fig. 2. In this model, the cylinder is filled with the medium identical to that out of the cylinder rather than a cavity, and therefore the whole domain is composed of a homogeneous medium. A heat source shaped in a cylindrical surface of a radius r_0 is buried in the medium with its axis being coincident with z -axis. The thickness, mass and heat capacity of the heat source are neglected. The heating rate per length of the cylindrical source, q_l , is constant since a starting instant, $\tau = \tau'$. The 2-D model for the smaller depth-to-diameter ratio of the pile was also developed to investigate the axial heat flow in our previous work.

As discussed in our previous paper [14], the temperature rise caused by an infinite “solid” cylindrical heat source at any location of the coordinate (r, z) and at the instant τ can be obtained according to the Green function theory as:

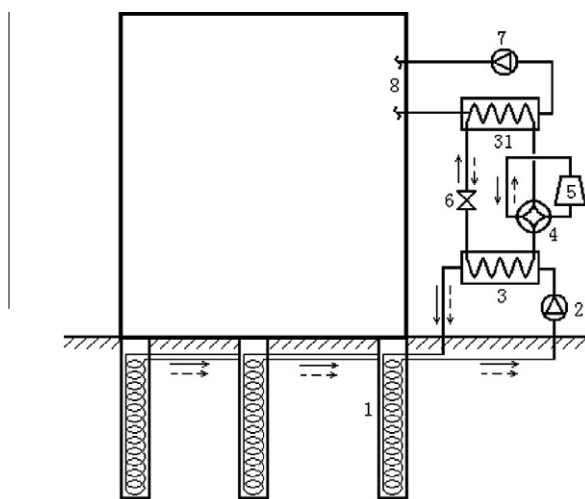


Fig. 1. Schematic diagram of a GCHP system with PGHEs.
 (1. PGHE; 2,7. circulation pump; 3,31. condenser and evaporator;
 (2. 4. reversing valve; 5. compressor; 6. expansion valve;
 (3. 8. conditioned space)

Fig. 1. Schematic diagram of a GCHP system with PGHEs.

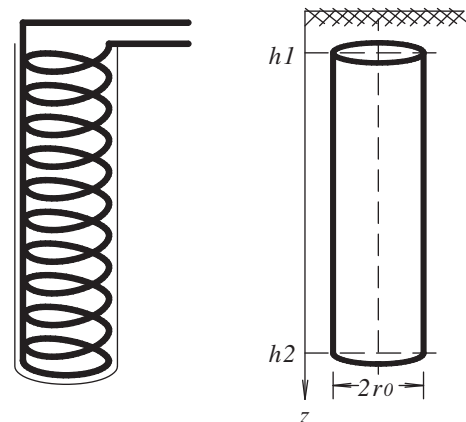


Fig. 2. Schematic diagram of the PGHE (left: spiral coils; right: finite “solid” cylindrical source model).

$$\theta_{c,i} = \frac{q_l}{4\pi k} \int_0^\tau \frac{1}{\tau - \tau'} \exp \left[-\frac{r^2 + r_0^2}{4a(\tau - \tau')} \right] \cdot I_0 \left[\frac{rr_0}{2a(\tau - \tau')} \right] d\tau' \quad (1)$$

where $I_0(x) = \frac{1}{\pi} \int_0^\pi \exp(x \cos \varphi') d\varphi'$ is the modified Bessel function of the zero order, $\theta_{c,i} = t_{c,i} - t_0$ is the temperature excess.

In the 2-D model, the cylindrical heat source is considered with a limited length, stretching from $h1$ to $h2$ in the Z direction. The image method was used to obtain the solution of this problem [14], as below:

$$\begin{aligned} \theta_{c,f} = & \frac{q_l}{8\pi k} \int_0^\tau \frac{1}{(\tau - \tau')} I_0 \left[\frac{rr_0}{2a(\tau - \tau')} \right] \exp \left[-\frac{r^2 + r_0^2}{4a(\tau - \tau')} \right] \\ & \cdot \left\{ \operatorname{erfc} \left[\frac{z - h2}{2\sqrt{a(\tau - \tau')}} \right] - \operatorname{erfc} \left[\frac{z - h1}{2\sqrt{a(\tau - \tau')}} \right] \right. \\ & \left. + \operatorname{erfc} \left[\frac{z + h2}{2\sqrt{a(\tau - \tau')}} \right] - \operatorname{erfc} \left[\frac{z + h1}{2\sqrt{a(\tau - \tau')}} \right] \right\} d\tau' \quad (2) \end{aligned}$$

While the “solid” cylindrical source model has made marked progress from the classical line source or “hollow” cylindrical source models, it fails to distinguish the effect of the spiral pitches because the coil is simplified as a continuous cylindrical surface. In practice, the temperature distribution fluctuates significantly along the axial direction in the vicinity of the cylindrical surface due to the non-integrity of the heat source. This feature is of great importance in analyzing the temperature rise of the buried pipe, and then, the circulating fluid in it. As a result, new models are needed for better understanding and analyzing the heat transfer around a buried coil.

An advanced model is established in this paper, and solved analytically to better describe the heat transfer process of the PGHE with spiral coils. Thus, the main objective of this study is to provide a more accurate algorithm which can be further used to calculate the temperature of the fluid in the spiral coil pipes and design the PGHE systems.

2. Ring-coil heat source model and solutions

An advanced model, i.e. the ring-coil source model, is proposed to take into account the discontinuity of the heat source and the impact of the coil pitches. The spiral coils buried in the pile are simplified as a number of separated rings on the cylindrical surface

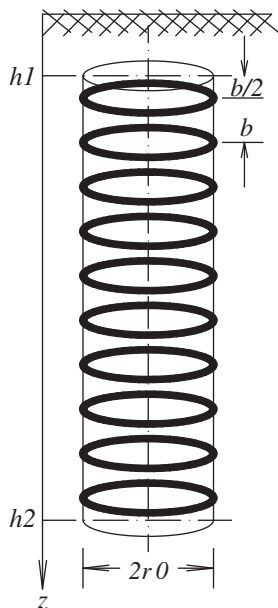


Fig. 3. The finite ring-coil source model.

of a radius r_0 with the pitch b being coincident with z -axis, as shown in Fig. 3. In order to analyze the thermal effect of the heat transfer along the axis on the total heat transfer efficiency, both the infinite and finite ring-coil source models are discussed in this paper.

The analysis on the heat transfer around the buried ring-coil pipes are based on the following assumptions.

- (1) The ground is regarded as a homogeneous medium, both inside and outside the cylindrical circumference; and its thermophysical properties do not change with temperature.
- (2) The medium has a uniform initial temperature, t_0 .
- (3) The ring-coils are assumed to be numerous ring-coil heat sources. Each of them emits heat at the intensity of $q_l b$ since a starting instant $\tau = \tau'$. The thickness, mass and heat capacity of the heat source are neglected.

For the ring-coil source model of finite length additional assumptions are taken:

- (4) The ground is assumed to be a semi-infinite medium, and its boundary, i.e. the ground surface, keeps a constant temperature t_0 (same as its initial one) throughout the period concerned.
- (5) The ring coils, are buried perpendicular to the boundary, stretching from depth $h1$ to depth $h2$.

2.1. Temperature response by a single ring-coil heat source

To develop the analytical model of the spiral coils, studying a single ring-coil heat source is the basic and simple starting point and then introducing other complications step by step. The ring coil is supposed to be located on the plane $z = z'$ with its axis being coincident with z -axis. It emits a continuous heating rate of q since a starting instant, $\tau = \tau'$.

Based on the governing equation of the transient heat conduction along with the given boundary and initial conditions, the two-dimensional heat conduction problem in the infinite medium can be formulated in the cylindrical coordinate:

$$\begin{aligned} \frac{\partial \theta}{\partial \tau} = & a \left(\frac{\partial^2 \theta}{\partial r^2} + \frac{1}{r} \frac{\partial \theta}{\partial r} + \frac{\partial^2 \theta}{\partial z^2} \right) + \frac{q \delta(r-r_0, z-z')}{2\pi r_0 \rho c}, & \text{for } 0 < r < \infty, -\infty < z < \infty, \tau > \tau' \\ \theta = & 0, & \text{for } 0 < r < \infty, -\infty < z < \infty, \tau = \tau' \\ \frac{\partial \theta}{\partial r} = & 0, & \text{for } r = 0, -\infty < z < \infty, \tau > \tau' \\ \theta \rightarrow & 0, & \text{for } r \rightarrow \infty, -\infty < z < \infty, \tau > \tau' \\ \theta \rightarrow & 0, & \text{for } z \rightarrow \pm \infty \end{aligned} \quad (3)$$

Thus, the temperature response at the location (r, z) in the medium to such a single ring source can be obtained according to the Green's function theory [15,16]:

$$\begin{aligned} \theta_{r,s} = & \frac{q}{2\pi \rho c} \int_0^\tau d\tau' \int_0^{2\pi} G d\varphi' \\ = & \frac{q}{8\rho c} \int_0^\tau \frac{1}{[\pi a(\tau - \tau')]^{3/2}} \\ & \times \exp \left[-\frac{r^2 + r_0^2 + (z - z')^2}{4a(\tau - \tau')} \right] I_0 \left[\frac{rr_0}{2a(\tau - \tau')} \right] d\tau' \quad (4) \end{aligned}$$

where the Green's function in the cylindrical coordinates is given as:

$$G = \frac{1}{8[\pi a(\tau - \tau')]^{3/2}} \cdot \exp \left[-\frac{r^2 + r_0^2 - 2rr' \cos(\varphi - \varphi') + (z - z')^2}{4a(\tau - \tau')} \right] \quad (5)$$

By introducing the following dimensionless variables: $\Theta = \frac{k\theta}{q}$, $Fo = \frac{\alpha\tau}{r_0^2}$, $Fo' = \frac{\alpha\tau'}{r_0^2}$, $R = \frac{r}{r_0}$, $Z = \frac{z}{r_0}$, $Z' = \frac{z'}{r_0}$, the dimensionless temperature excess at (R, Z) can be expressed as a function of the following dimensionless variables:

$$\Theta_{r,s} = \frac{1}{8\pi^{3/2}} \int_0^{Fo} \frac{1}{(Fo - Fo')^{3/2}} I_0 \left[\frac{R}{2(Fo - Fo')} \right] \times \exp \left[-\frac{R^2 + 1}{4(Fo - Fo')} \right] \exp \left[-\frac{(Z - Z')^2}{4(Fo - Fo')} \right] dFo' \quad (6)$$

2.2. Infinite ring-coil source model

The infinite ring-coil source model is firstly studied, which means that the ring-coil source is assumed to be infinite in the longitudinal direction. The z -coordinates of the ring coils are defined to be $z' = \pm (n + 0.5)b$, where $n = 0, 1, 2, \dots, +\infty$. As a consequence, the overall temperature response at a random point in the medium to all the ring sources can be determined as the sum of all the individual temperature rises caused by each ring-coil source.

$$\begin{aligned} \theta_{r,i} &= \frac{q_1 b}{2\pi\rho c} \left(\sum_{n=-\infty}^0 \int_0^\tau d\tau' \int_0^{2\pi} G(z' = nb - 0.5b) d\varphi' \right. \\ &+ \left. \sum_{n=0}^{\infty} \int_0^\tau d\tau' \int_0^{2\pi} G(z' = nb + 0.5b) d\varphi' \right) \\ &= \frac{q_1 b}{8\rho c} \sum_{n=0}^{\infty} \int_0^\tau \frac{1}{[\pi a(\tau - \tau')]^{3/2}} I_0 \left[\frac{rr_0}{2a(\tau - \tau')} \right] \\ &\times \left\{ \exp \left[-\frac{r^2 + r_0^2 + (z - nb - 0.5b)^2}{4a(\tau - \tau')} \right] \right. \\ &+ \left. \exp \left[-\frac{r^2 + r_0^2 + (z + nb + 0.5b)^2}{4a(\tau - \tau')} \right] \right\} d\tau' \quad (7) \end{aligned}$$

After introducing another dimensionless variable of $B = \frac{b}{r_0}$, Eq. (7) can be rewritten in the dimensionless format:

$$\begin{aligned} \Theta_{r,i}(R, Z, Fo) &= \frac{B}{8\pi^{3/2}} \sum_{n=0}^{\infty} \int_0^{Fo} \frac{1}{(Fo - Fo')^{3/2}} I_0 \left[\frac{R}{2(Fo - Fo')} \right] \\ &\times \exp \left[-\frac{R^2 + 1}{4(Fo - Fo')} \right] \left\{ \exp \left[-\frac{(Z - nB - 0.5B)^2}{4(Fo - Fo')} \right] \right. \\ &+ \left. \exp \left[-\frac{(Z + nB + 0.5B)^2}{4(Fo - Fo')} \right] \right\} dFo' \quad (8) \end{aligned}$$

2.3. Finite ring-coil source model

The effects of heat flow through the top and bottom ends of the pile are neglected in the above infinite model, and therefore it is inadequate for the long-term operation of the PGHE especially in view of the much smaller depth-to-radius ratio of the pile than that of the borehole. While keeping the ring-coil source simplification, the spiral coil is taken as a finite ring-coil source buried in a semi-infinite medium, stretching from h_1 to h_2 from the boundary of the ground surface. The coil is then approximated as m pieces of rings, where $m = \text{int} [(h_2 - h_1)/b]$. Again, the images of the ring coils with negative heating rate $-q_1 b$ are set on symmetry to the boundary in order to keep the constant temperature of the ground surface, and the solution for the ring-coil source model of finite length is expressed as:

$$\begin{aligned} \theta_{r,f} &= \frac{q_1 b}{2\pi\rho c} \int_0^\tau d\tau' \left[\sum_{n=0}^m \int_0^{2\pi} G(z' = h_1 + nb + 0.5b) d\varphi' \right. \\ &- \left. \sum_{n=0}^m \int_0^{2\pi} G(z' = -h_1 - nb - 0.5b) d\varphi' \right] \\ &= \frac{q_1 b}{8\rho c} \int_0^\tau \frac{1}{[\pi a(\tau - \tau')]^{3/2}} I_0 \left[\frac{rr_0}{2a(\tau - \tau')} \right] \cdot \exp \left[-\frac{r^2 + r_0^2}{4a(\tau - \tau')} \right] \\ &\cdot \sum_{n=1}^m \left\{ \exp \left[-\frac{(z - h_1 - nb - 0.5b)^2}{4a(\tau - \tau')} \right] \right. \\ &- \left. \exp \left[-\frac{(z + h_1 + nb + 0.5b)^2}{4a(\tau - \tau')} \right] \right\} d\tau' \quad (9) \end{aligned}$$

Define $H1 = \frac{h_1}{r_0}$ and $H2 = \frac{h_2}{r_0}$, then Eq. (9) can be rewritten as follows:

$$\begin{aligned} \Theta_{r,f}(R, Z, Fo) &= \frac{B}{8\pi^{3/2}} \int_0^{Fo} \frac{1}{(Fo - Fo')^{3/2}} I_0 \left[\frac{R}{2(Fo - Fo')} \right] \\ &\times \exp \left[-\frac{R^2 + 1}{4(Fo - Fo')} \right] \\ &\times \sum_{n=0}^m \left\{ \exp \left[-\frac{(Z - H1 - (n + 0.5)B)^2}{4(Fo - Fo')} \right] \right. \\ &- \left. \exp \left[-\frac{(Z + H1 + (n + 0.5)B)^2}{4(Fo - Fo')} \right] \right\} dFo' \quad (10) \end{aligned}$$

3. Comparisons and discussion

3.1. Comparisons of infinite and finite ring-coil source models

The temperature responses of the infinite and finite ring-coil source models can be calculated easily according to Eqs. (8) and (10), respectively, and the computation results are illustrated in Figs. 4 and 5.

Taking an example of infinite ring-coil source with $B = 1$, the temperature distributions at the cylindrical surfaces of $R = 1$, $R = 0.5$ and $R = 1.2$ along the Z direction are described in Fig. 4. In general, the temperature rises fluctuate considerably in the vicinity to the ring-coil sources and shows a periodic variation in the Z direction, which is due to the discontinuity of the ring-coil sources in the longitudinal direction. The temperature at the cylindrical

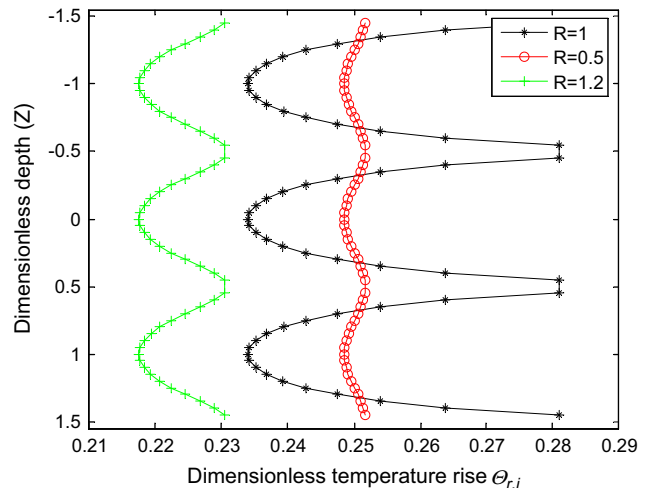


Fig. 4. Temperature distribution along the Z -axis with different R as parameter ($B = 1$, $Fo = 10$).

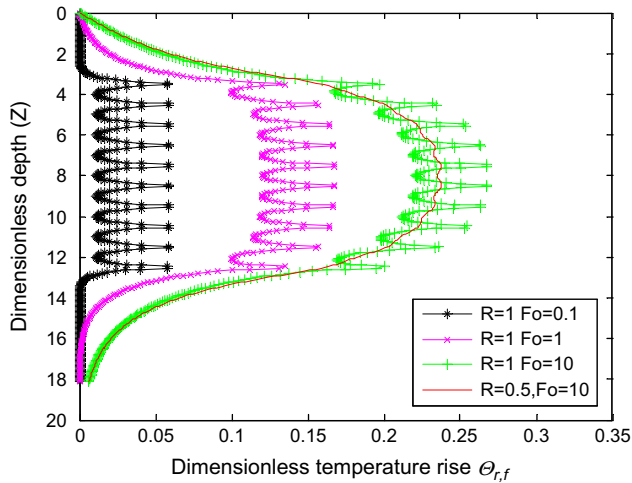


Fig. 5. Temperature profiles along the pile depth with different Fo (with $H1 = 2$, $H2 = 12$, $B = 1$).

surface of ring coils with $R = 1$ appears an extraordinary fluctuation, and tends to infinity at locations, where the ring sources exist.

For a PGHE with $H1 = 2$, $H2 = 12$, and $B = 1$, the temperature responses on the cylindrical surface of the ring-coil source (i.e. $R = 1$) along the pile depth at different instants (Fo) are computed and plotted in Fig. 5. As shown in Fig. 5, for the case of $Fo = 0.1$, the temperature distribution at $R = 1$ shows a quite similar periodic variation to that of the infinite model (as seen in Fig. 4) except points near the top and bottom ends of the pile. This indicates that the influence of the axial heat conduction caused by the boundary and finite length of the heat source is limited to the two ends of the pile in relatively short periods of time. For long-term operation, however, the impact of heat dissipation through the ends will penetrate deeper into the whole depth of the pile, and then the significant deviations from the temperature distribution of the infinite model occur, as shown in Fig. 5.

Even though the temperatures in both the infinite and finite ring-coil models vary with time and pile depth, as shown in Figs. 4 and 5, the radical differences between them increase with the time elapses, especially for long-term periods. In view of the comparisons between the two models, the temperature at the mid-point of two ring-coil sources on the cylindrical surface of $R = 1$ is chosen as a representative one. For the infinite ring-coil model, the tem-

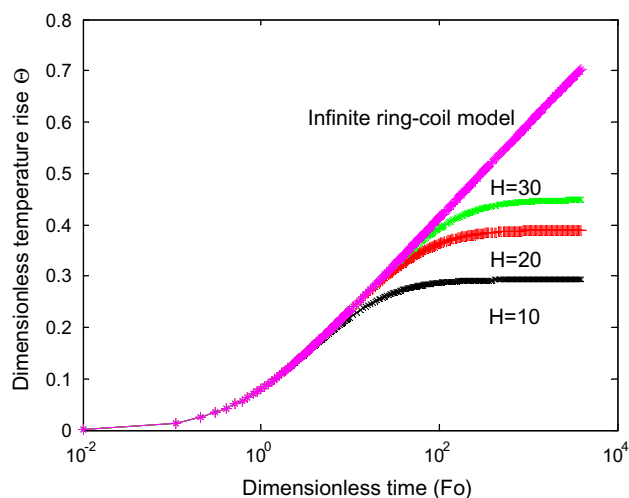


Fig. 6. Dimensionless temperatures vs. Fo from finite and infinite ring-coil models.

perature at the point with $R = 1$ and $Z = 0$ is taken as the representative temperature of the coil surface. For the finite model, the temperature at the middle of the pile depth ($R = 1$, $Z = (H2 + H1)/2$) is computed for comparison purpose.

The representative temperatures calculated from the two models are illustrated in Fig. 6. In general, the infinite model yields a relatively higher temperature response compared with the finite model because of its neglect of the heat transfer through the top and bottom ends of the pile. The infinite ring-coil model results in a good agreement with the finite model for a short initial period, but remarkable discrepancy of the infinite model from the finite one appears due to the assumption of the infinite heat source with respect to long-term duration. Obviously, the shorter the pile is the larger discrepancy between them occurs. When the time tends to infinity, the temperature response of the infinite model also tends to infinity as the finite model reaches a steady-state one which corresponds to the actual heat transfer mechanism. This feature demonstrates the importance to take the length effect into account regarding the long-term operation of the PGHEs. In the PGHE applications, the depth-to-diameter ratio of the heat source is usually much smaller than that of the vertical boreholes, so the finite heat source model should be employed in the thermal analysis of the PGHEs.

3.2. Comparisons of infinite ring-coil source and “solid” cylindrical source models

The ring-coil source model becomes the “solid” cylindrical model when $B = 0$, where the temperature distribution is independent of Z coordinate for the case of infinite heat source. Fig. 7 compares the temperature distributions along the radial direction of infinite ring-coil source and the infinite “solid” cylindrical source ($B = 0$) models with different parameters of Z and B . It can be seen from Fig. 7 that the two models show a similar trend of the temperature variation along the radial direction. Each temperature profile from the two models reaches an apex at the circumference of the heat source, i.e. $R = 1$, at any Z -level, and heat flows, then, to both sides of the cylindrical circumference.

The temperature distribution of the ring-coil model fluctuates along the Z direction because of the discontinuous ring coils. As shown in Fig. 7, the temperature rise at the Z -level away from the ring coil may be lower than that of the cylindrical model, such as $Z = 0$, whereas, the temperature rise near the ring-coil source exhibits a higher value than that of the cylindrical model. The

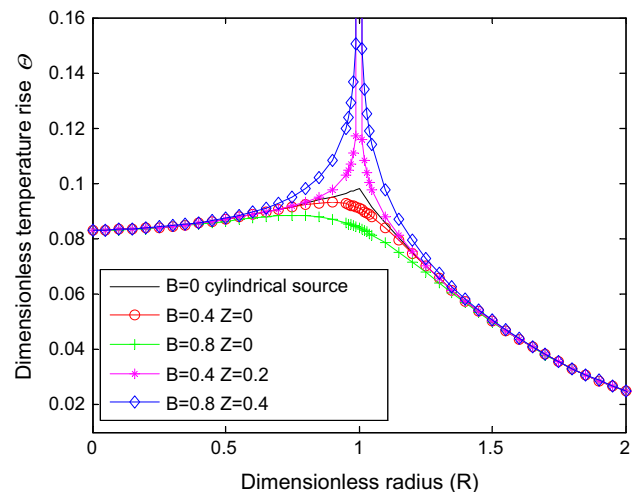


Fig. 7. Temperature profiles along radial direction with different Z and B values ($Fo = 1$).

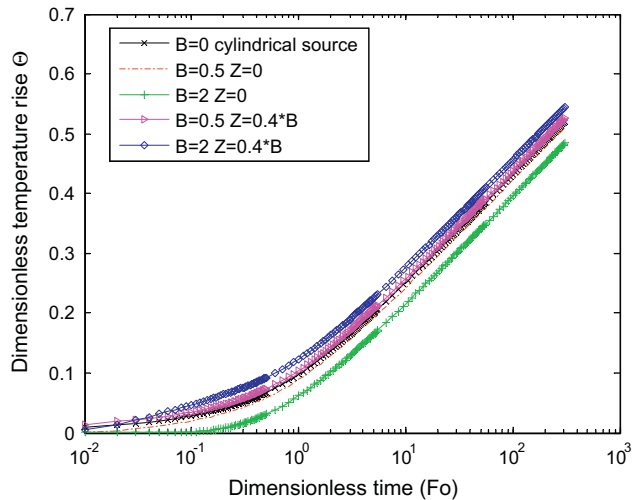


Fig. 8. Comparisons of temperature responses on the cylindrical surface of $R = 1$ from infinite ring-coil and cylindrical sources with different pitches.

highest temperature rise occurs in the plane of $Z = 0.4$, where the ring-coil source is located, and the temperature obtained from the ring-coil model at $R = 1$ tends to infinite due to the assumption of the line source nature of the rings.

Fig. 7 also depicts different temperature profiles with different coil pitches in order to better investigate the effect of the ring-coil density on the temperature distribution along the axis direction. It gives that the deviation of the cylindrical model from the ring-coil model dramatically increases with the rise in the coil pitch for the same heat intensity per length of the coils. For a smaller pitch, such as $B = 0.4$, the temperature profile of the ring-coil model is closer to that of the “solid” cylindrical model. This means that the “solid” cylindrical model can be accepted for the cases with dense ring coils. In addition, the temperature deviation between the two models shows a maximum value on the cylindrical surface of ring coils, where $R = 1$, and then rapidly attenuates at locations away from the heat sources in the radial direction. This demonstrates that the influence of pitch on the temperature response can be neglected at the locations far away from the heat source in a short term period.

Fig. 8 compares the variations of the temperature rises on the cylindrical surfaces of $R = 1$ for the two models with the time elapses. Since the cylindrical heat source can be reckoned as a collection of numerous ring-coil heat sources with a same heating intensity per length as the ring-coil source model, there is no temperature difference along the Z direction for this model. Consequently, Fig. 8 demonstrates that the temperature rise from the ring-coil source is much larger in the vicinity of the ring sources and slightly smaller near the middle points of the ring coils compared with those of the cylindrical model. However, in the design of the PGHEs in GCHP systems, special attention should be paid to the temperature rise on the pile wall, where is quite close to the ring coils. As a result, a significant error may be caused by the cylindrical model in calculating the temperature rise on the pile wall. Thus, it is essential to employ the ring-coil heat source model to design the PGHEs more accurately.

3.3. Comparisons of finite cylindrical and ring-coil source models

Fig. 9 compares the temperature distributions along the pile depth obtained from the finite cylindrical and ring-coil source models respectively. Basically, the temperature rises of the ring-coil source model fluctuate around the temperature profiles of

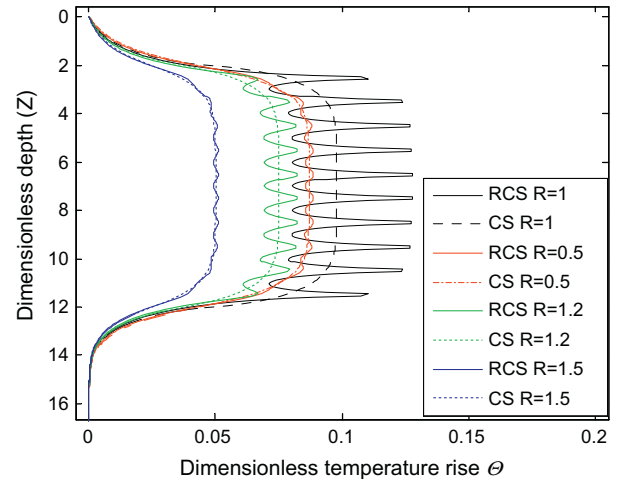


Fig. 9. Comparisons of temperature profiles along pile depth between finite cylindrical and ring-coil source models (where RCS = ring-coil source and CS = cylindrical source; $H_1 = 2$, $H_2 = 12$, $B = 1$, $Fo = 1$).

the cylindrical model with large amplitude near the ring coil, and the amplitude of the fluctuation gradually abates away from the cylindrical surface of the ring coil in the radial direction.

According to the computation results and the comparisons, it is obvious that the ring-coil model can better describe the heat conduction in the PGHEs with spiral coils compared with the “solid” cylindrical model owing to its more realistic assumptions.

4. Conclusions

Based on the “solid” cylindrical heat source model, an improved analytical model of ring-coil heat source is established to better illustrate the heat transfer process of the PGHE with spiral coils. In the ring-coil source model, the discontinuity of the heat source is considered, and the impact of the coil pitch is investigated by introducing more appropriate approximations of the real coil. In this model, the buried coils are simplified as a number of separated rings on the cylindrical surface with the pitch b . In order to investigate the impacts of the ground surface and the limited length of the PGHEs, both the infinite and the finite-length heat source models are developed and their analytical solutions are derived according to the Green’s function theory and the image method. Both the temperature distributions for the two models and the impact of the coil pitch on the thermal process are discussed respectively for comparison based on the simulation results.

The simulation results give that the infinite ring-coil model may be acceptable for engineering applications for short-time system operation. However, for long-term duration, it is vital to consider the heat conduction through the two ends of the pile, especially for the pile with smaller depth-to-diameter ratio.

Comparisons between the cylindrical and ring-coil models indicate that the temperature rises of the ring-coil source model remarkably fluctuate around the temperature profiles of the cylindrical model, with larger amplitude near the ring coil and smaller one far away the ring coil. In conclusion, the ring-coil source model of finite length can describe the heat conduction in the PGHEs with spiral coils more accurately compared with both the infinite ring-coil and cylindrical source models.

It should be pointed out that the dimension of the coil pipe is still neglected in the models and is assumed to be a ring-coil heat source. As a result, the temperature on the points, where the ring sources locate, tends to infinity, which deviates from the realistic conditions. Fortunately, it is still applicable in practice as the tem-

perature rises on the pipe wall which is desirable for GHE design in the engineering applications is at certain distance away from the ring source. Though the ring-coil source models can better describe the heat transfer process of the spiral coils and take the spiral pitch into account, they still show a deviation from the practical heat transfer problem due to its assumption of spiral coil as ring-coil. The application and experimental verification of the simulation model presented here will be addressed soon in a separate paper.

Acknowledgements

The research is supported jointly by a Grant from Shandong Province Natural Science Foundation, China (Project No. ZR2010EQ006) and a Grant from Shandong Jianzhu University (010180902).

References

- [1] Spitler JD. Ground-source heat pump system research past, present and future. *HVAC and R Res* 2005;11(2):165–7.
- [2] Yu MZ, Diao NR, Su DC, Fang ZH. A pilot project of the closed-loop ground-source heat pump system in China. *Proc IEA 7th Heat Pump Conf* 2002:356–64.
- [3] Morino K, Oka T. Study on heat exchanged in soil by circulating water in a steel pile. *Energy Build* 1994;21(1):65–78.
- [4] Pahud D, Fromentin A, Hadorn JC. The duct ground heat storage model (DST) for TRNSYS used for the simulation of heat exchanger piles. *DGC-LASEN, Lausanne*; 1996.
- [5] Pahud D, Fromentin A, Hubbuch M. Heat exchanger pile system for heating and cooling at Zurich Airport. *IEA Heat Pump Centre Newsletter*. 1999;17(1):15–6.
- [6] Laloui L, Nuth M, Vulliet L. Experimental and numerical investigations of the behaviour of a heat exchanger pile. *Int J Numer Anal Methods Geomech* 2006;30(8):763–81.
- [7] Yasuhiro Hamada, Hisashi Saitoh, Makoto Nakamura, Hideki Kubota, Kiyoshi Ochifuji. Field performance of a PGHE system for space heating. *Energy Build* 2007;39(5):517–24.
- [8] Sekine K, Ooka R, Yokoi M, Shiba Y, Hwang S. Development of a ground-source heat pump system with ground heat exchanger utilizing the cast-in-place concrete pile foundations of buildings. *ASHRAE Trans* 2007;113(PART 1):558–66.
- [9] Bose JE, Parker JD, McQuiston FC. Design/data manual for closed-loop ground-coupled heat pump systems. Atlanta: American Society of Heating Refrigerating and Air-Conditioning Engineers; 1985.
- [10] Eskilson P. Thermal analysis of heat extraction boreholes. Doctoral Thesis, Department of Mathematical Physics, University of Lund, Sweden; 1987.
- [11] Yavuzturk C, Spitler JD, Rees SJ. A transient two-dimensional finite volume model for the simulation of vertical U-tube ground heat exchangers. *ASHRAE Trans* 1999;105(2):465–74.
- [12] Zeng HY, Diao NR, Fang ZH. A finite line-source model for boreholes in geothermal heat exchangers. *Heat Transfer Asian Res* 2002;31(7):558–67.
- [13] Kavanaugh SP. Simulation and experimental verification of vertical groundcoupled heat pump systems. Doctoral Thesis Oklahoma State University: Stillwater, Oklahoma; 1985.
- [14] Man Y, Yang HX, Diao NR, Liu JH, Fang ZH. A new model and analytical solutions for borehole and pile ground heat exchangers. *Int J Heat Mass Trans* 2010;53:2593–601.
- [15] Jia L, Fang ZH. *Advanced heat transfer*. Beijing: China Higher Education Press; 2008.
- [16] Beck J, Cole K, Haji-Sheikh A, Litkouhi B. *Heat conduction using Green's functions*. Hemisphere 1992.